Synthesis and physicochemical characterization of Zn-2,4-dichlorophenox acetate
layered nanohybrid and controlled release properties

تخليق وتشخيص فيزيائي كيميائي للتهجين النانوي لطبقة الزنك ٢-٤داي كلورو فينوكسي خلات وخواص عملية التحرر المسيطر عليها .

Abbas Matrod- Bashi

Department of chemistry, faculty of science, Karbala University

الخلاصة //

تفاعل اوكسيد الخارصين مع ٢,٤داي كلورو فينوكسي حامض الخليك لتكوين(زنك-٢٤د) الطبقي في اتمـام التهجين النانوي مما اكد ذلك التشخيص بالأشعة السينية الذي اظهر بصورة واضحة تركيب بلوري نانوي منتظم في طورين الاول عند ٢٥,٢ انكستروم والثاني عند ٢٤ انكستروم. كذللك تشخيص الميكروسكوب الالكترونـي الماسح والنافذ والـذي اظهر شكلا مشابها لشكل الوردة والذي يتاثر بشكل كبير بتركيز ٢,٤دايكلوروفينوكسي خـلات المستعمل. اظهرت دراسـات السيطرة علـئ التحرر بانه ٩٤% منه بشكل كبير وذلك في غضون ساعتين، كذلك يظهر ان عملية التنافذ تتحكم فـي عمليـة التحرر، العمليـة كليا تخضع لقانون الرتبة الثانية الكاذبة احركيا.

Abstract

Reaction of ZnO with 2,4-Dichlorophenoxy acetic acid (24D) for the formation of a Zn-24D-layered nanohybrid (ZDN), was accomplished . Powder X-ray Diffractogram shows a well ordered crystalline nanomaterial in two phases with a spacing 25.2, and 24 Å. SEM and TEM studies show a flower-like morphology which is highly effected by the concentration of the 24D used. The release studies showed a rapid release of 94% of 24D for the first 100 min. which govern by the inter particle diffusion pseudo second order was found to govern the release of 24D from ZDN. This study suggests controlled release formulation.

Key words**:** Nanocomposite, 2,4-dichlorophenoxy acetic acid, zinc oxide layer nanohybrid, controlled release.

1.0 Introduction

The increasing use of the agrochemicals in agricultural activities is the main processes leading toward water contamination, which made them a primary source of water pollution. One approach to reduce pesticide transport losses is to use controlled release formulations, Useful effects related to the use of controlled release formulations system planned take account of reductions in the quantity of chemical required for control. Decrease in the risk of direct use and environmental pollution in which the pesticide is encapsulate into a matrix or carrier before application, in that way limiting the unwanted losses of this chemicals. The interactions between matrix and the active pesticide is trapped otherwise sorbed into an inert support are important and is gradually release in excess of time. Several natural and synthetic material have been proposed for use in pesticide controlled release formulation, such as the lamella of Zn-Al-layered double hydroxide intercalated with naphthaleneacetate to forming a nanocomposite [1]., several papers talk about the synthesis of ZnO and its structure characterization, but few of them study the intercalations of ZnO such as a new paper Zinc-layer-gallate was synthesis [2] also the effect of polymers onto the size of zinc layered hydroxide salt and its calcined product was study [3], in other side many publications on anionic and cationic clay mineral have been widely used for this purpose as supports for the controlled release of herbicides, such as the acids herbicides removal by calcined Mg-Al-CO3-LDH acid herbicides[4]. The organohydrotalcites as novel supports for the slow release of the herbicide terbuthylazine [5]. Adsorption of acidic pesticides 2,4-D, Clopyralid and Picloram on calcined hydrotalcite [6]. Adsorption of MCPA pesticide by MgAl-layered double hydroxides [7].

Montmorillonitephenyltrimethylammonium yields environmentally improved formulations of hydrophobic herbicides [8].

Zinc Oxide nanoparicles received considerable attention due to its wide potential in the technical applications in various scientific area of science and technology like antibacterium [9], gas sensor [10], dye-sensited solar cell [11] carbon nonofibers were prepared by Carbonization of ZnO coated by polyacrylonitril [12], also the effect of a conjugated polymer with ZnO have been preparation and studied [13]. Controlled release technologies have emerged as an approach to solve the problem of contamination with herbicides used as plant growth regulator by synthesis of LDH-nanocomposites in this laboratory[14, 15], new article on the uses of LDH as supports for intercalation and sustain release of antihypertensive drugs[16]. A new research work reported here focusing on the method of synthesis of zinc-24D layered nanohybrid by of ZnO with 24D and physicochemical investigations of the structure morphology of the resulted ZDN and its controlled release in carbonate media.

2.0 Materials and Methods

ZnO purchesed from ACrose, 2,4-chlorophenoxy acetic acid (24D) from Merck, were use without farther purification. Solusion of (0.05, 0.1, 0.2, 0.4 M 24D were prepared by dissolving in 50ml of 90 % ethanol. The solution was added to 0.5gm ZnO in a conical flask, under N_2 gas, stirred for two hours, aging at 70°C for 18 hours, cooled, centrifuged and wash for four times with deionized water, dried in oven at 70 ^{o}C, grinding and kept in a sample bottle for further analyses.

3. 0 Characterizations

Powder X-Ray Diffraction patterns (PXRD) were obtained with a Shimadzu XRD-6000 powder diffractometer using (λ=1.540562 Å) at 40 kV and 30 mA a scan rate of 0.5 min./degrees

Fourier Transform Infrared (FTIR) spectra were recorded by using a spectrophotometer thermo Nicolet Ft-IR Nexus self supporting sample in the range of 4000-400 cm^{-1}. The CHNS analyzer, model CHNS-932(LECO) was used to determine the percentage of and 24D, and the TG/DTG were carried out with a Setaram TG-DSC-11 apparatus with fully programmable heating and cooling sequence sweep gas valve switching and data analysis. The surface morphology and bulk structure of the sample were observed by scanning electron microscope (SEM) model JOEL (JSM-6400).and TEM Hitachi (H 7100).

3.1 Results and Discussion

3.1.1 XRD Powder x-ray diffraction

Powder X-ray diffraction patterns of ZnO nanoparticles and Zn-layered hydroxide in direct intercalated with 24D are shown in Fig. [1]. All the nanomaterials show sharp and high intensity diffracted patterns, with well ordered and highly crystalline was observed material. As result of the intercalation of 24D anion an expansion of the basal spacing of ZnO showed. This is due to the size and spatial orientation of the anion in the inorganic interlayer's of Zn-layered hybride.
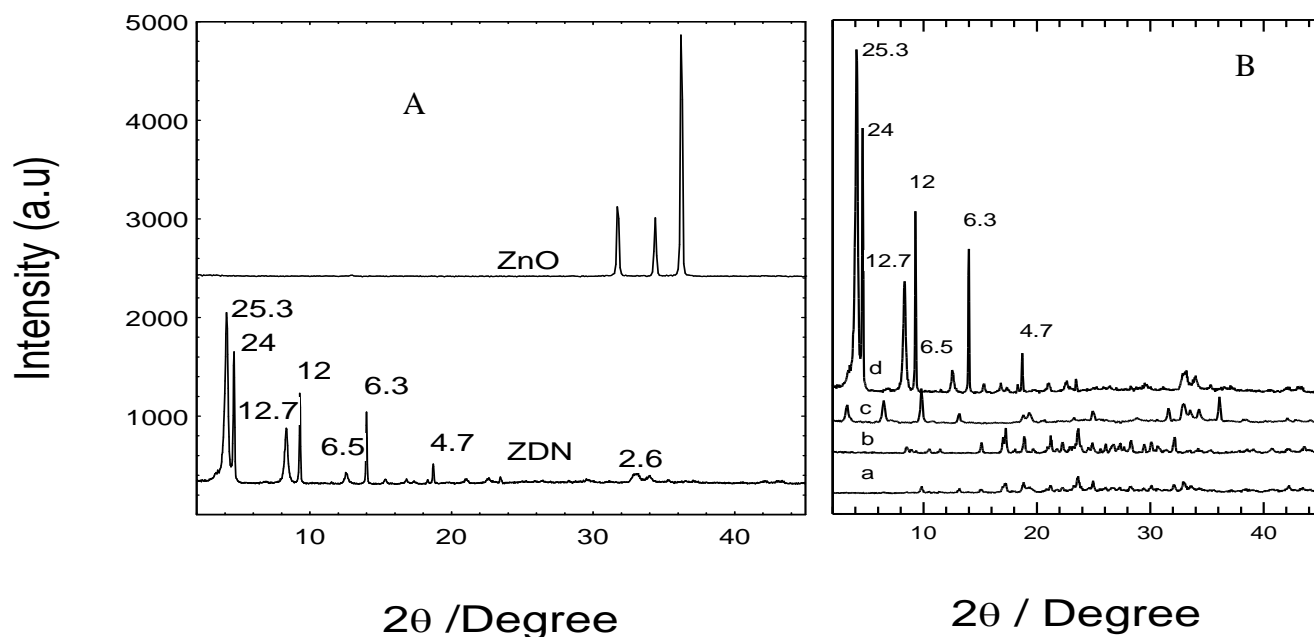
Fig.[1A] shows the pattern of ZnO(top) and zinc-24D-layered nanohybrid, .[1B] evolution of structure morphology of zinc-24D-layered with initial concentrations of 24D, a(0.05), b (0.1), c(0.2) and d(0.4) M .

Zinc-layered 24D nanohybrid shows well ordered biphasic nanohybrid with the interlayer of 003 and 006, is 25.2 Å and 12.7Å for the first phase and that of the second phase are 24 Å and 12 Å. Respectively. These new peaks do not exist on the XRD pattern of ZnO. The crystallinity of the resulting materials is depending on the initial concentration of 24D. Increasing concentration of the anion gives well ordered XRD pattern specially the evolution of the phase with d 003 at about 25.2 Å, with the increasing initial concentration resulting, Fig[1B] shows the development of the crystal growth from a monophase fig.[1B], patterns [a, b, c], to two different phases pattern [d], with increasing initial concentrations of 24D. This is a characteristic of intercalations host-guest type. SEM and TEM image showed the development of the crystal shape at low initial concentration of 24D (0.05 M), this structure became flowerlike -structure with the material initial 24D concentrations at (0.4 M). This indicates that 24D find its own way and assemble itself for the formation of nanohybrids, resulting in the formation of well-defined ZDN nanophase nanohybrid. The chloride ion in the mixture media plays a role as competitor ion and because of its small size compared to the 24D ion it is easy to diffuse to the interior of the particles of ZnO, and opened an easy means to be followed by the 24D ion. so that makes the nanoparticle ZDN more homogenous and highly crystalline. At the same time no change in the peaks characteristic to ZnO planes pattern at 2.65 ,2.60 and 2.47 ^{o}A positions although the intensities was reduced with comparing to the high intense patterns of ZDN after intercalation of ZnO with 24D Fig.[1A]. SEM and TEM shows that the original layers of ZnO still kept their original structure.

3.1.2 SEM Morphology

The as-prepared ZDN shows flowered like-structure with various sizes and shapes. The morphology of ZDN and ZnO samples is different depending on the synthesis parameters. Fig [2] shows SEM photomicrographs of (B,C,D) for ZCN, (C) for ZnO and TEM images Fig. 2 [E, F,G and H] for ZDN. The development of the grown flower- like morphology of ZDN samples synthesized by using a series of concentrations E(0.05 M), F (0.1 M) G (0.2 M) and H (0.4 M). These samples shows that with increasing concentration of 24D, more agglomeration takes place. The layered structure formation started with initial concentration of 24D between 0.05 - 0.2 M fig.

[2B], E, F, G, and H showing flowering growth. That is very regular straight sheet was obtained when the initial concentration reach 0.4 M. As shown in SEM Fig.[, (D). The XRD pattern also shows that within this range of concentration development of second phase of d003 at about 25.2Å was obtained more ordered and further symmetric, so that the second phase of d003 at 24 Å. The resulted ZDN well ordered white crystallized nanoparticles which is a general character for crystal growth showed by SEM micrographs ZCN a micro-flowered morphology with non uniform size distribution of flowered structure. Within the range of initial concentration between 0.05 - 0.2 M. We can affirm here that the concentration of 24D is an important factor that Controlling the homogeneity and the growth of two phases nanocomposites biphasic. It may be the orientation of one molecule of 24D assembling its self with the layers of ZnO. Or probably the molar ratio 24D/ZnO in the solution play an important role in the intercalations processes. The resulting intercalated ZDN nano structure with high crystal quality is very important for the application researches in nanocomposite controlled release.
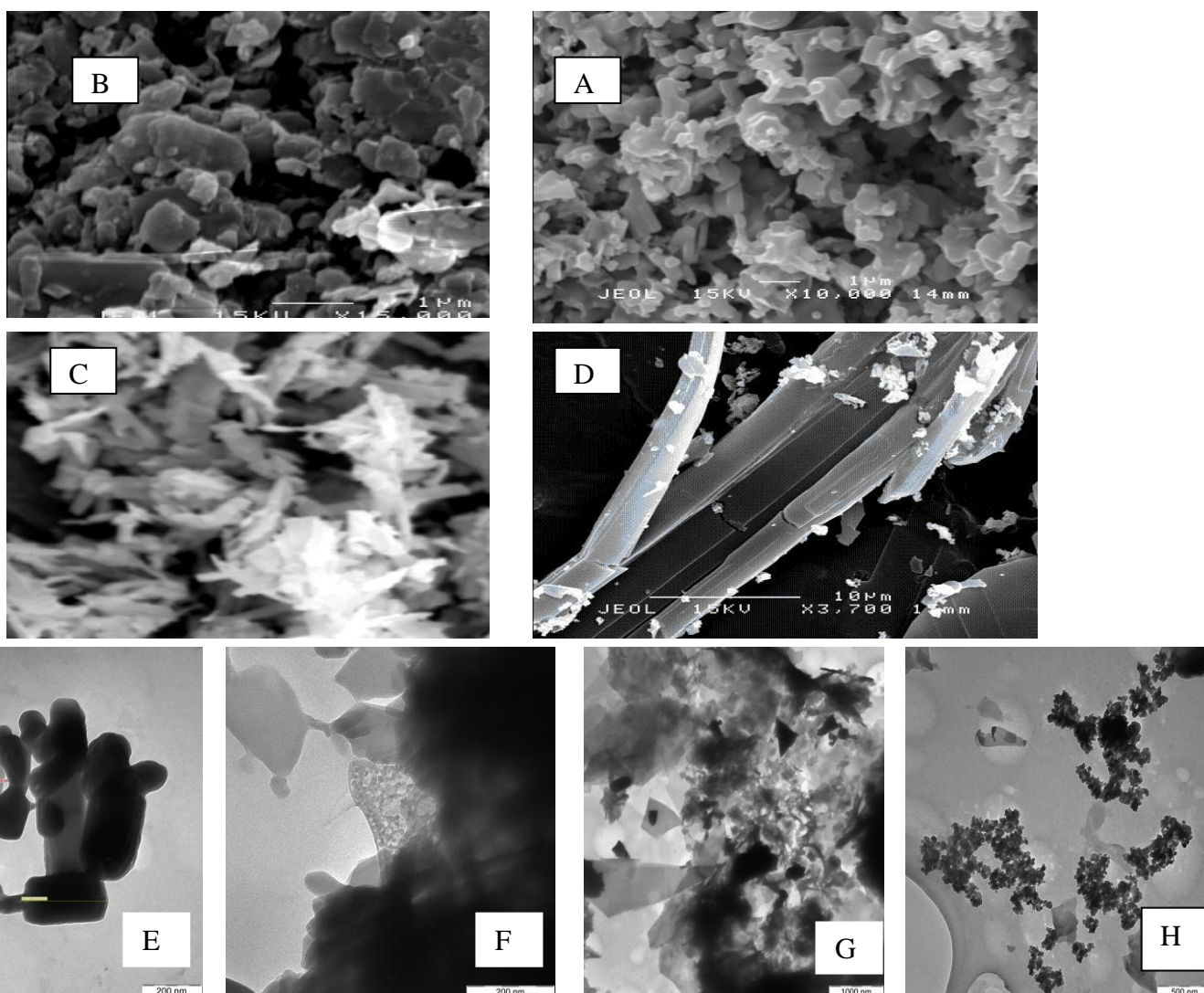

Fig [2A] shows SEM of ZDN after intercalation with 24D at initial concentration, A (ZnO non intercalated) B (0.05M), C(0.1M) and D (0.4M).
Fig.[2B] shows TEM images at initial concentrations of 24D, E (0.05M), F (0.1M), G (0.2M) and H(0.4M).

. 3.1.3 FTIR Technique

The presence of the herbicide anion in the nanohybrid can be verified by Fourier Transform Infrared Spectroscopy (FTIR). Fig. [3] presents the infrared spectra of ZnO, ZDN and 24D. The broad absorption bands at 3455 cm^{-1} is due to the stretching vibrations mode of OH groups in the Zinc-hydroxide layer and physisorbed water. The shoulder at 3369 cm^{-1} shows the existence of hydrogen bonding between the water molecules and the Zinc-hydroxide layer,or between water molecules and the anion 24D. The band at 1615cm^{-1} assigned to stretching vibrations of water molecule. The band at 2930cm^{-1} is attributed to C–H stretching vibration of the intercalated 24D (from CH_2COO^- group), A peaks at 1546 and 1326 cm^{-1} are assigned to antisymmetric and symmetric stretching vibrations of the (-COO-) group. The bands observed at around 1487 and 1441 cm^{-1} attributed to the C=C bond of the aromatic ring in 24D.
The (C-O-C) anti symmetric and symmetric stretching vibrations bands appear at 1220 and 1067 cm^{-1}.
A band observed at 829 cm^{-1} corresponding to (-CH_2) rocking.
  The bands in the lower wavenumber region (i.e., 400–800 cm^{-1}) are due to M–O and M–OH bending vibration in the ZnO layers that can be seen in FTIR spectrum of ZDN and ZnO.. All of this indicates that was accruals 24D intercalated in the ZnO interlayer.
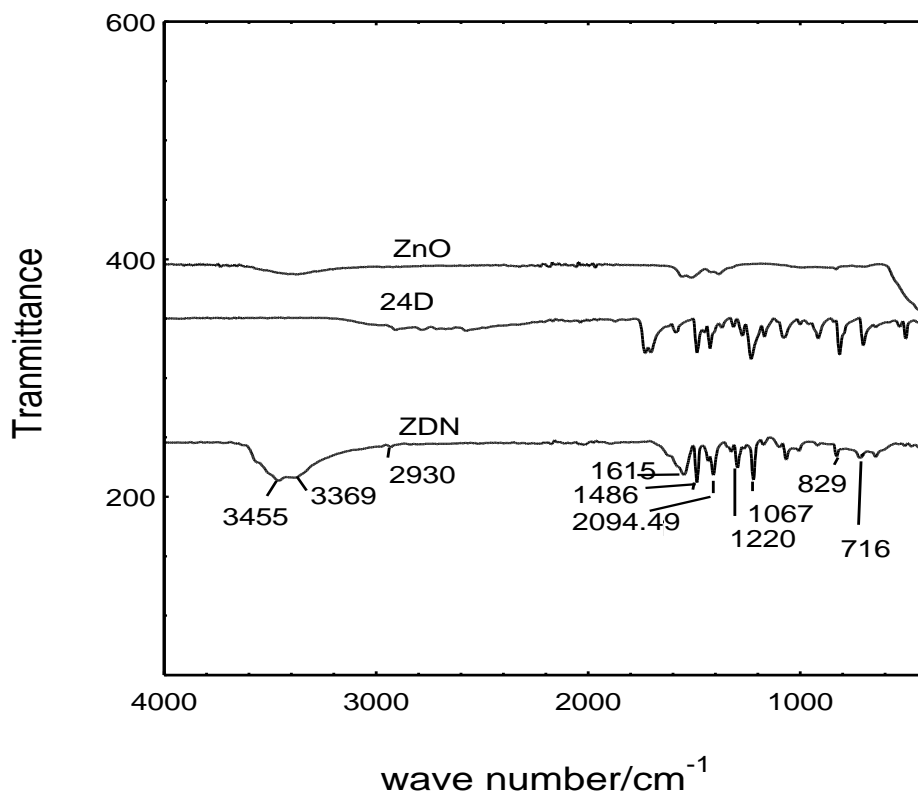

Fig [3] FTIR spectrum of ZDN, 24D and ZnO shows the characteristic peaks.

3.1.4 UV Energy Gap
The energy band gap of ZnO nanoparticle (ZDN). Is shown in FIG. [4] showing high optical transmittance above 70 % within the range of 400-800 nm. The optical transmittance at wavelength of 256 nm E_{gap} = 4.85 eV. can be obtained. The E_{gap} shifted to 4.71 eV within increase 24D ion concentration. At 316 nm E_{gap} was 3.92 eV see table[1] This absorption shifted to 319-328 nm when the ion concentration reach 0.4 M, in this state E_{gap} = 3.78eV. The absorption edge of ZnO film also shifted to a shorter wavelength. This phenomenon indicates that the optical energy gap is enlarged

with the increase in ion concentration loaded by ZnO to create a ZDN as we had shown in the XRD and SEM morphology. The blue shift adsorption edge is due to the increase of 24D concentration and so the optical energy gap see table [1] .
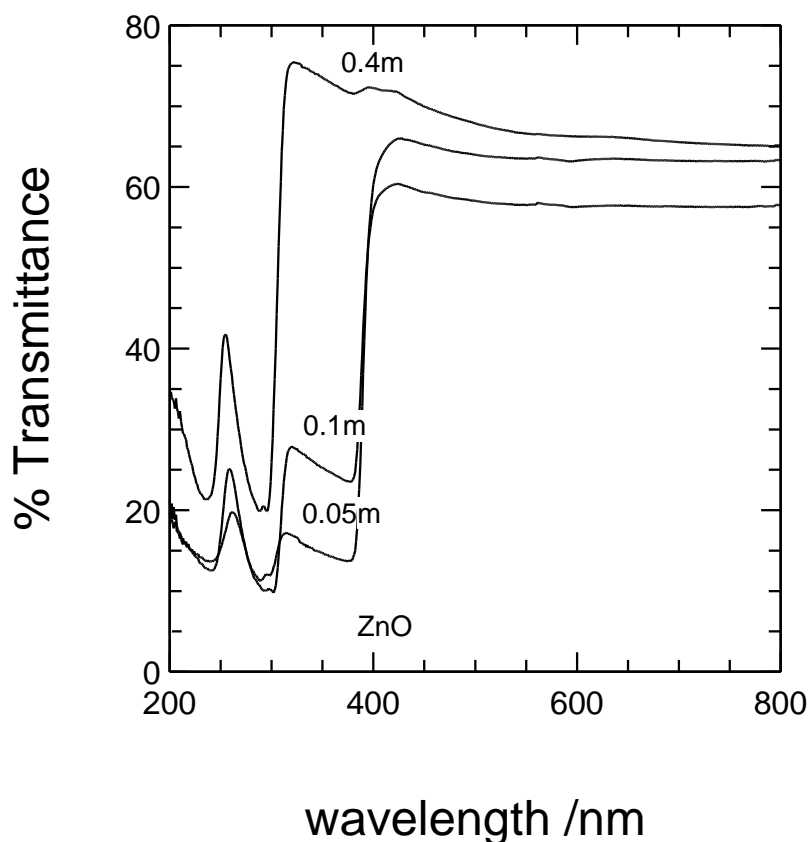

Fig [4] UV.-VIS. Energy gap from low to up, 0.05, 0.1, 0.2 and 0.4 M of 24D loaded by ZDN.

3.1.5 Thermal Analysis

Fig. [5] shows the TG-DTG curves of ZDN also the table [1] listed the details of the TG, reveal three distinguishable weight loss steps. The first steps indicate a losses of 9.67 % started from 37 ^{o}C terminating at 168 ^{o}C with maximum temperature of 138 ^{o}C this is attributed to the loss of physical adsorbed water in the interlayer. The next stage with total loss = 35.3 % at the temperature between (250-396) ^{o}C and peak maximum at 314 ^{o}C, is due to the decomposition and subtle combustion of 24D. The third phenomenon is endothermic with total loss of about 2.3 %, between (492-593) ^{o}C with a peak maximum of 541 ^{o}C which is due to the strong to combustion of 24D. The total loss achieved is around 47.3%.
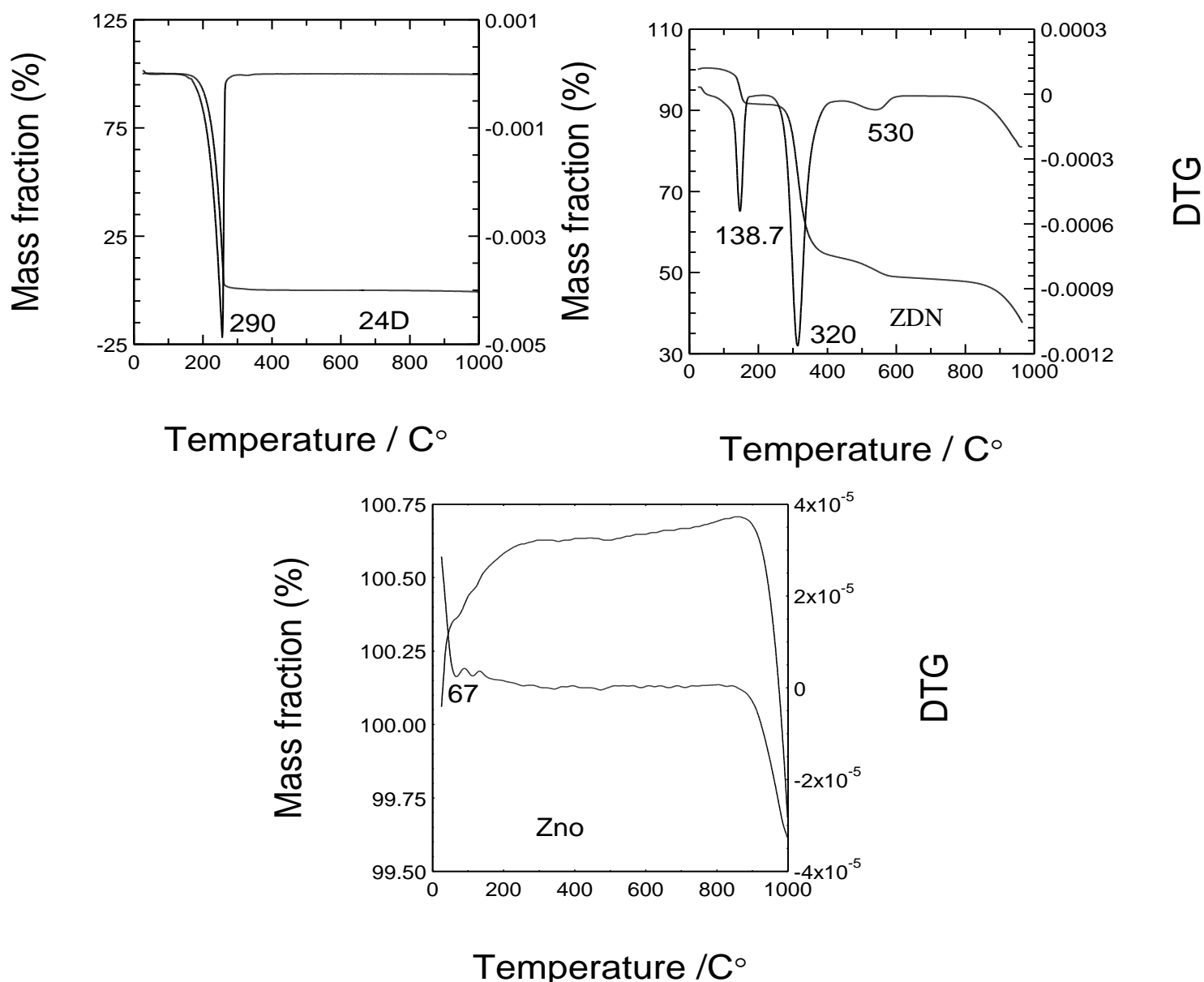
Figure [5] TG-DTG analysis of 24D, ZDN and ZnO standard.

3.1.6 Kinetic Study

The release profile of 24D from the inter layer of ZnO (ZDN) in to aqueous solution is at the concentration 0.005 M sodium carbonate. The accumulated 24D release into the aqueous solution is 94 % within 100 minutes and this is the equilibrium stage of release fig.[6A]. The release was fitted to different equations. Fig.[6], [B] zero- order, [C] first order, [D] pseudo second order and [E] parabolic diffusions between 0-1500 min. The release was found to governed by the pseudo second order equation as indicated by r^2 value which is 0.999. With t $_{1/2}$ of 220, table [1] show the parameter of of the kinetic study.
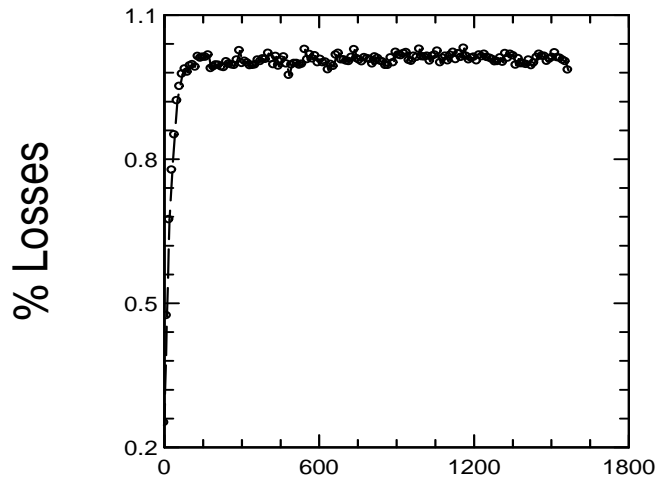
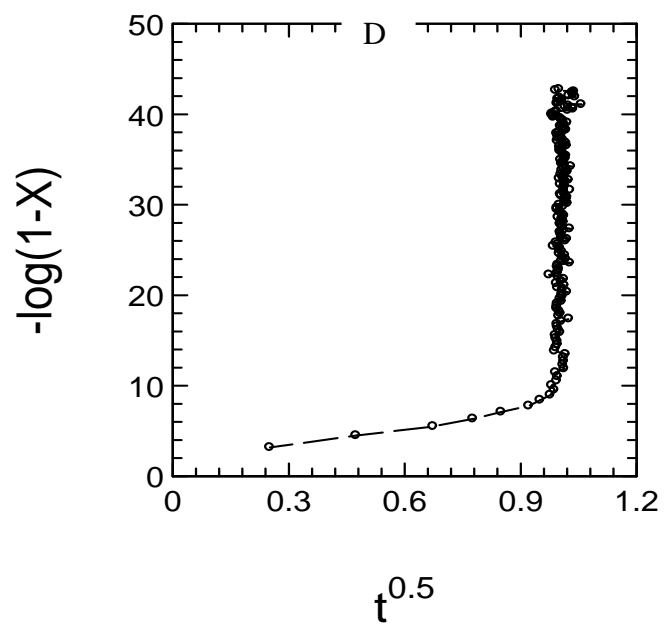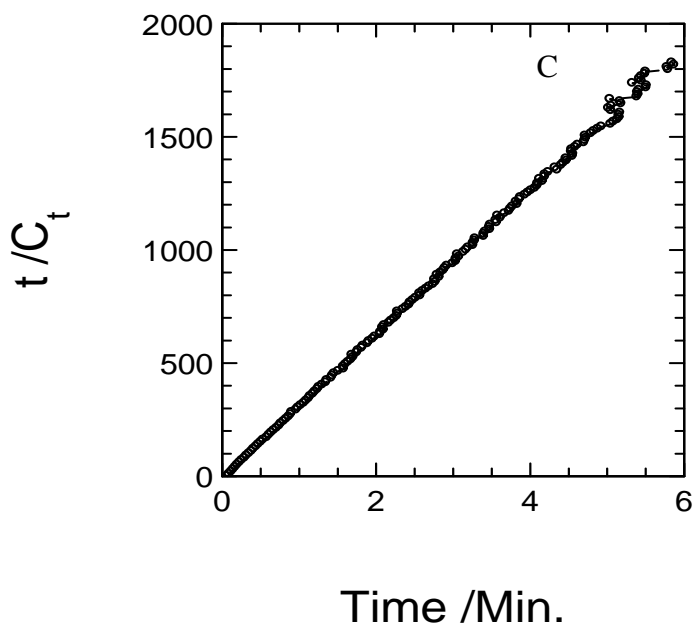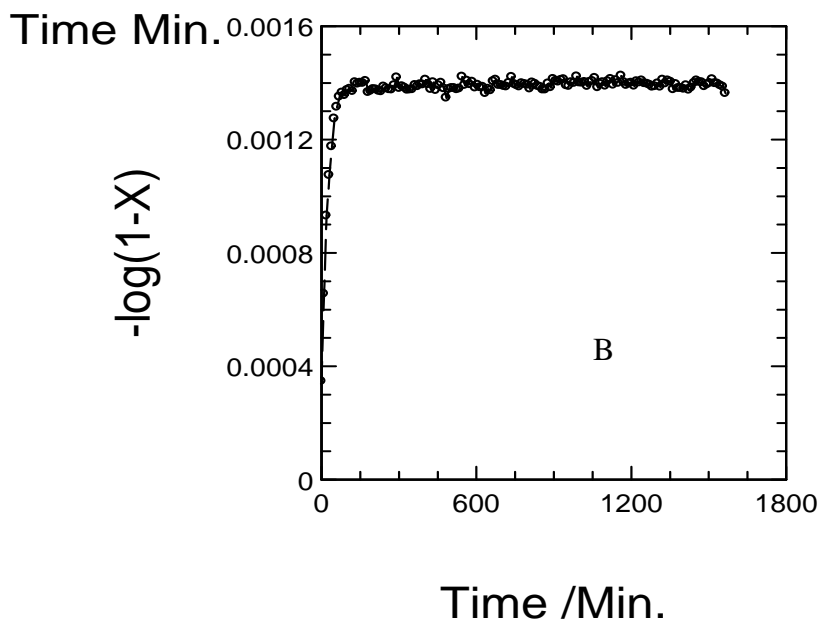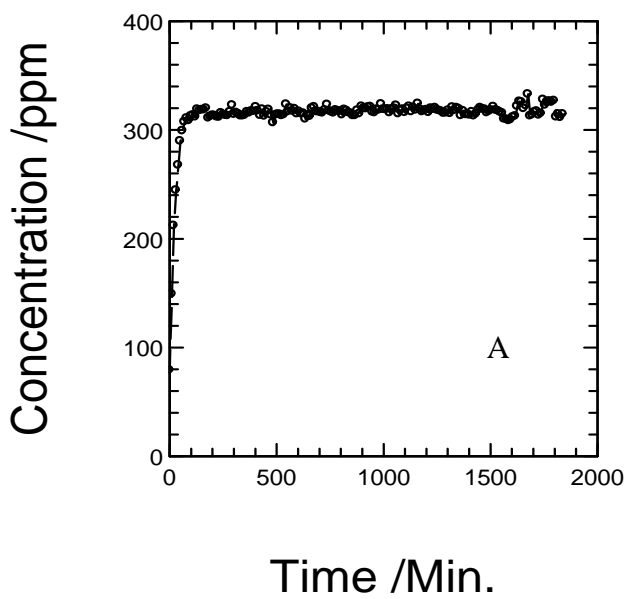Fig. [6A] release % of 24D from the inter lamellar space nanocomposite Zn-24D.

Fig [6B] % Release, (A), 1st Order (B) pseudo second order (C) and the module of parabolic diffusion(D).

4.0 Conclusion

A new nanohybrid material which shows controlled release capabilities with 24D molecule intercalated into Zinc layered interlamellae as a guest and 24D was obtained using direct reaction of ZnO and 24D. The resulting material has a very well ordered crystalline layered nanocomposite. The release of the 24D anion from the interlamellae of the organic-inorganic nanohybrid material was found to be of controlled manner.

Release of 24D ions from the interlamellae of the nanocomposite is due to the ion exchange process and the dissolution of the layered inorganic Zinc. This happened fairly rapidly even after one hour contact time and it was also found that the release of 24D anions from the interlamellae of ZDN with carbonate as incoming anion could be better described by the pseudo second order equation than zero and the first order kinetic. The diffusion rate is the main factor that governed the release of 24D at the beginning of the release, which is completed within one hour contact times.

5.0 References

[1] M. Z. Hussien, Z. Zainal, A. H. Yahya, D.W.V. Foo, Controlled release of a plant regulator, naphthaleneacetate from the lamella of Zn-Al-layered double hydroxide nanocomposite, J. Control. Release 82 (2002)417-427

[2] M. Z. Husseina, M. Ghotbi, A. H. Yahaya, M. Z. Abd Rahman, Synthesis and characterization of (zinc-layered-gallate) nanohybrid using structural memory effect, Mater. Chem. Phys. 113 (2009) 491–496

[3] M. Z. Hussein, M. Y. GhotbiA. H. Yahaya and M. Z. Abd Rahman, The effect of polymers onto the size of zinc layered hydroxide salt and its calcined product, doi:10.1016/j.solid state sciences.2008.006

[4] L. P. Cardoso, J. B. Valim, Study of acids herbicides removal by calcined Mg—Al—CO3—LDH. J. Physi. Chem. Solid 67 (2006) 987–993.

[5] F. Bruna, I. Pavlovic, R. Celis, C. Barriga, J. Cornejo, M.A. Ulibarri, Organohydrotalcites as novel supports for the slow release of the herbicide terbuthylazine, Appli. Clay Sci. 42 (2008) 194–200.

[6] I. Pavlovic, C. Barriga, M. C. Hermosı´n, J. Cornejo, M. A. Ulibarr, Adsorption of acidic pesticides 2,4-D, Clopyralid and Picloram on calcined hydrotalcite, Appli. Clay Sci. 30 (2005) 125– 133.

[7] J. Inacio, C. Taviot-Gue´ho, C. Forano, J. P. Besse, Adsorption of MCPA pesticide by MgAl-layered double hydroxides, Applied Clay Science 18 (2001) 255–264.

[8] Y. El-Nahhal, S. Nir, C. Serban, O. Rabinovitch, B. Rubin, Montmorillonitephenyltrimethylammonium yields environmentally improved formulations of hydrophobic herbicides. *J. Agric. Food Chem. 48*(200) 4791-4801.

[9] L. Zhang, Y. Ding, M. Povey, D. York, ZnO nanofluids – A potential antibacterial agent. Progres. Nat. Sci. 18 (2008) 939–944.

[10] M. R. Vaezi, SnO_2/ZnO double-layer thin films: A novel economical preparation and investigation of sensitivity and stability of double-layer gas sensors. Mater. Chem. Phy. 110 (2008) 89–94.

[11] S. Rani, P. Suri , P. K. Shishodia, R. M. Mehra, Synthesis of nanocrystalline ZnO powder via sol–gel route for dye-sensitized solar cells. Sol. Energy Mater. Sol. Cells (2008), doi:10.1016/j.solmat.2008.07.015

[12] L.Y. Lin, H. J. Kim, D. E. Kim, Wetting characteristics of ZnO smooth film and nanowire structure with and without OTS coating. Appl. Sur. Sci. 254 (2008) 7370–7376.

[13] M. Wang, Y. Lian, X. Wang, PPV/PVA/ZnO nanocomposite prepared by complex precursor method and its photovoltaic application. Curr. Appl. Phys. 9 (2009) 189–194.

[14] M. Z. Hussein, S. H. Sarijo, A. Yahya, Z. Zainal, J. Nanosci. Nanotechnol.7 (8) (2007)2852-2862.

[15] M. Z. Hussein, Z. Zainal, A. Yahaya, and H. K. Loo, Sci. Technol. Adv. Mater. 6(2005)956.

[16] S. J. Xia, Z. M. Ni, Q. Xu, B. Gu, J. Hu, Layered double hydroxides as supports for intercalation and sustained release of antihypertensive drugs, J. solid stat.chem. (2008), doi:10.1016/j.jssc.2008.06.009.